Published in final edited form as:
Stem Cells. 2009 November ; 27(11): 2804–2814. doi:10.1002/stem.215.

Multi-pathway Kinase Signatures of Multipotent Stromal Cells are Predictive for Osteogenic Differentiation

Manu O. Platt[1,*], **Catera L. Wilder**[1], **Alan Wells**[2], **Linda G. Griffith**[1], and **Douglas A. Lauffenburger**[1]

[1]Department of Biological Engineering, Massachusetts Institute of Technology, Cambridge MA 02139

[2]Department of Pathology, University of Pittsburgh and Pittsburgh VAMC

Abstract

Bone marrow-derived multi-potent stromal cells (MSCs) offer great promise for regenerating tissue. While certain transcription factors have been identified in association with tendency toward particular MSC differentiation phenotypes, the regulatory network of key receptor-mediated signaling pathways activated by extracellular ligands that induce various differentiation responses remain poorly understood. Attempts to predict differentiation fate tendencies from individual pathways in isolation are problematic due to the complex pathway interactions inherent in signaling networks. Accordingly, we have undertaken a multi-variate systems approach integrating experimental measurement of multiple kinase pathway activities and osteogenic differentiation in MSCs, together with computational analysis to elucidate quantitative combinations of kinase signals predictive of cell behavior across diverse contexts. In particular, for culture on polymeric biomaterials surfaces presenting tethered epidermal growth factor (tEGF), type-I collagen, neither, or both, we have found that a partial least-squares regression model yields successful prediction of phenotypic behavior on the basis of two principal components comprising the weighted sums of 8 intracellular phosphoproteins: p-EGFR, p-Akt, p-ERK1/2, p-Hsp27, p-c-jun, p-GSK3α/β, p-p38, and p-STAT3. This combination provides strongest predictive capability for 21-day differentiated phenotype status when calculated from day-7 signal measurements (99%); day-4 (88%) and day-14 (89%) signal measurements are also significantly predictive, indicating a broad time-frame during MSC osteogenesis wherein multiple pathways and states of the kinase signaling network are quantitatively integrated to regulate gene expression, cell processes, and ultimately, cell fate.

Keywords

Biomathematical modeling; Bone marrow stromal cells; Cell signaling; Mesenchymal stem cells; Stem cell-microenvironment interactions

Corresponding Author: D.A. Lauffenburger, 16-343 MIT, 77 Massachusetts Avenue, Cambridge MA 02139, 617-252-1629 (telephone), 617-258-0204 (fax), lauffen@mit.edu.
*current address: Wallace H. Coulter Department of Biomedical Engineering at Georgia Tech and Emory University, Atlanta GA 30332

Author contributions:

Manu O. Platt: conception and design, financial support, collection and/or assembly of data, data analysis and interpretation, manuscript writing, and final approval of manuscript
Catera L. Wilder: collection and/or assembly of data
Alan Wells: financial support, data analysis and interpretation, final approval of manuscript
Linda G. Griffith: conception and design, financial support, data analysis, manuscript writing, and final approval of manuscript
Douglas A. Lauffenburger: conception and design, financial support, data analysis and interpretation, manuscript writing, and final approval of manuscript

INTRODUCTION

Bone marrow-derived multi-potent stromal cells (MSCs) are versatile progenitor cells capable of differentiating into bone, cartilage, and fat cells[1–3] with potential for regenerative medicine applications. Epidermal growth factor receptor (EGFR)-mediated signaling has been implicated in many steps of MSC proliferation and bone regeneration[4–7]. We have previously shown that tethering EGF to polymeric substrates to physically inhibit endocytosis of the EGF-EGFR complex elicits sustained EGFR activity[8, 9] and increased osteogenic differentiation of MSCs compared to control surfaces when induced by osteogenic media[10]. Activation of EGFR is also associated with enhanced proliferation of the stem or progenitor cell compartment without impairing differentiation[4, 7], or even enhancing differentiation under osteogenic conditions[5], but elucidation of the signaling networks linking EGFR to bone differentiation is incomplete. In fact, many signals downstream of EGFR are contested in literature regarding their positive or negative influences on MSC osteogenic differentiation. Both inhibition and activation of ERK and MAPK signaling have been shown to increase osteogenesis in MSCs and pre-osteoblasts[11–13]. Conflict around PI3K/Akt, another major signaling molecule and pathway which may be preferentially activated by tEGF restricting EGFR signaling to the plasma membrane[14, 15], includes reports showing that activation[16–19] and inhibition[5] increase osteogenic differentiation. GSK3α/β and p38 MAPK interact with MAPK and PI3K pathways, both positively and negatively, to inhibit or activate Runx2, the master osteogenic transcription factor – further confounding the total picture[20–25] of an individual pathway's effect on osteogenic differentiation.

These disputed effects may arise from univariate examination of progenitor cell differentiation signals especially since these pathways integrate at the level of activation of ubiquitous kinases such as ERK, Akt, JNK, STAT, p38, and GSK3α/β (Supplementary Fig 1), which participate in osteogenic differentiation programs, activated by various ligands, soluble factors, and cues. MSCs must integrate multiple cues from the microenvironment and neighboring cells to make decisions about differentiation and proliferation. Computational analysis of the dynamic changes in kinase activation has shown that kinases act as integrators of cue information to produce specific cellular responses[26, 27]. Importantly, prediction of cell phenotypic behavior across diverse contexts and treatment conditions is substantially improved when multiple pathways are considered in concert, rather than any single particular signaling pathway. In such studies, systematic variation of extracellular cues across a landscape of conditions allows a broad range of signaling network activities to be considered.

Herein we accordingly employ a multi-variate, quantitative systems approach to understand how various kinase pathways work together to govern osteogenic differentiation of MSCs across a number of biomaterial conditions, examining outcomes from culture on polymeric substrates presenting tEGF and/or Collagen-I. Our signaling measurements target kinases previously implicated either in differentiation or proliferation and known to be activated by a spectrum of stimuli: EGFR (Tyr)[4, 5, 7, 28–32], ERK1/2 (Thr202/Tyr204, Thr185/Tyr187)[11, 13, 19, 33–37], Akt (Ser473)[16, 17, 19], p38 MAPK (Thr180/Tyr182)[13, 22, 23, 38–41], HSP27 (Ser78)[42], c-Jun (Ser63)[43–45], STAT3 (Ser727)[46], and GSK3α/β (Ser21/Ser9) [20, 21, 25, 47, 48]. Signals were measured after 1, 2, 4, 7, and 14 days of culture, and analyzed with respect to their predictive relationships to 21 day matrix mineralization, a marker of osteogenic differentiation, across all the diverse culture conditions.

Computational analysis was undertaken using partial least squares regression (PLSR), a data-driven modeling technique proven in previous work in other cell phenotypic fate decision studies to ascertain quantitative contributions of multiple signals to a measured cellular response[26, 27]. The PLSR model relates cellular kinase signals across multiple pathways (specifically: ERK, Akt, p38, JNK, GSK3, and STAT3) to 21-day matrix mineralization. We

find not only that a kinase 'network signature' quantitatively combining seven phospho-site levels on day 7 from this set of pathways successfully accounts for tEGF effects on day 21 mineralization, but also successfully predicts *a priori* both of two opposing effects of using adsorbed Collagen-I as a substrate for MSC culture relative to nonspecific adhesion: an increase in mineralization in the absence of tEGF, and a decrease in mineralization in the presence of tEGF. This latter finding addresses the challenge of extrapolating outcomes from individual cues/conditions to complex *in vivo* situations, demonstrating the utility of network signatures that integrate diverse inputs to provide predictive information.

MATERIALS AND METHODS

Cell culture

Primary human multi-potent stromal cells were obtained from Tulane Center for Gene Therapy, and maintained according to prescribed protocols. MSCs were expanded in α-MEM with L-glutamine and without ribonucleosides or deoxyribonucleosides (Invitrogen/GIBCO) supplemented with 16.5% fetal bovine serum (Atlanta Biologicals), L-glutamine (200 mM), and penicillin-streptomycin (100 units/ml -100 μg/ml). For osteogenic differentiation, medium was supplemented with 50 μM L-Ascorbic acid 2-phosphate, 20 mM β-glycerophosphate, and 10 nM dexamethasone.

Polymeric substrate preparation

Polymeric substrates were prepared as previously described[8] with one modification; control surfaces were prepared with the same 40:60 tEGF-polymer:diluent ratio as the tEGF surfaces, but phosphate buffer without EGF was used during the coupling procedure. For *in vitro* experiments, each substrate was placed in individual wells of a 12-well plate and seeded with ~25,000 cells/cm^2 (50,000 cells per well). After the culture period and treatments, prior to biochemical assay, surfaces were transferred to a new 12 well plate. Where indicated, substrates were coated with rat tail collagen I (BD Biosciences) in phosphate buffered saline by incubation in 1 μg/ml solution for one hour at room temperature, followed by 3 rinses in sterile phosphate buffered saline prior to biochemical assay.

Cell and protein quantification

Cell counts were determined using the CyQuant DNA assay (Invitrogen) according to manufacturer protocols. Total protein concentrations were determined using the BCA kit (Pierce).

Immunoassays for quantifying signaling protein phosphorylation

Bioplex® bead kits were used for phosphorylated EGFR determination (BioRad), and Novagen® bead kits were used for total EGFR determination (EMD Sciences) according to manufacturer's instructions with 10 μg protein from each sample. Bioplex assays were conducted for the following kinases: EGFR (Tyr)[4, 5, 7, 28–32], ERK1/2 (Thr202/Tyr204, Thr185/Tyr187)[11, 13, 19, 33–37], Akt (Ser473)[16, 17, 19], p38 MAPK (Thr180/Tyr182)[13, 22, 23, 38–41], HSP27 (Ser78)[42], c-Jun (Ser63)[43–45], STAT3 (Ser727)[46], and GSK3α/β (Ser21/Ser9) [20, 21, 25, 47, 48]. Signals were measured after 1, 2, 4, 7, and 14 days of culture. EGFR fluorescence values at each point were used to calculate absolute EGFR numbers using a standard curve generated with increasing concentrations of the extracellular domain of EGFR provided by the manufacturer (Novagen). Signal values for each different phosphorylated kinase were normalized to the value for that kinase in a master lysate prepared in bulk from MSCs stimulated with 1 ng/ml soluble EGF and exposed to UV for 30 minutes to activate different kinase pathways, separated into single thaw aliquots, and used with each experiment.

Signal values for each different kinase were then divided by the maximum value observed for that kinase over the entire experimental time period, thus scaling values between 0 and 1.

Statistical testing

Significance was determined using unpaired student's t-test. P values <0.05 were considered significantly different.

Partial Least-Squares Regression modeling

Raw data values from Bioplex analysis were first normalized to the master lysate (i.e., the time course data set for each kinase in the samples was divided by the reference value for that kinase in the master lysate). Resulting normalized values for each kinase were then normalized to the maximum value in the time course data set for that kinase, thus scaling all values between 0 and 1. This process was also used for the alkaline phosphatase activity assay, all quantitative RT-PCR, cell proliferation, and xMAP assays. To generate the PLSR model, SIMCA-P software (UMetrics) was used as described previously[49]; a detailed explanation of the approach is provided in the Supplementary Materials.

RESULTS

Tethered EGF influences cell proliferation and differentiation

In the context of regenerative medicine applications, proliferation and expansion of adult stem cells will be an important aspect prior to terminal differentiation. We have previously found that tEGF acts to enhance osteogenic differentiation of these MSCs[10] (Fig 1A), so broadened our assessment of tEGF effects by measuring increases in cell number for both undifferentiating and differentiating MSCs on tEGF or control surfaces (Fig 1B). MSCs were seeded onto 12-mm control or tEGF surfaces at a density of 25,000 cells/cm^2. MSCs were cultured in either expansion medium (Exp), which maintains the cells in an undifferentiated phenotype, or with osteoinductive supplements (OS) added 24 hours after seeding. There were a greater number of cells after 7 days in Exp medium compared to OS medium, and tEGF induced greater proliferation (Fig 1B; *p<0.05). Increases in MSC cell number halted in OS medium between 7 and 14 days of culture at cell confluence, but continued to increase through day 21 in Exp medium resulting in overlapping cell layers. By day 21, tEGF and control cell numbers were the same within a medium condition, perhaps due to contact inhibition of cell division.

Kinase signaling data-compendium reveals complex multi-pathway activities during osteogenic differentiation

To investigate how key signaling pathways govern the phenotypic behavior induced by tEGF, we measured dynamic signal activation profiles of MSCs on control and tEGF substrata under the Exp and OS conditions of Figure 1. Our signaling set was comprised of kinases implicated in literature reports as impacting MSC proliferation or differentiation, with activity level characterized by specific phosphorylation site status: EGFR (Tyr)[4, 5, 7, 28–32], ERK1/2 (Thr202/Tyr204, Thr185/Tyr187)[11, 13, 19, 33–37], Akt (Ser473)[16, 17, 19], p38 MAPK (Thr180/Tyr182)[13, 22, 23, 38–41], HSP27 (Ser78)[42], c-Jun (Ser63)[43–45], STAT3 (Ser727) [46], and GSK3α/β (Ser21/Ser9) [20, 21, 25, 47, 48]. Signals were measured after 1, 2, 4, 7, and 14 days of culture in either Exp or OS medium in the absence or presence of 1 μM AG1478, the EGFR kinase inhibitor; all assays consisted of at least biological triplicates. These data are displayed in Figure 2, enabling visual inspection of the diverse effects of tEGF and culture media on the various signaling pathway activities. We can identify that 1 μM AG1478 effectively inhibits EGFR phosphorylation with a subsequent effect on ERK 1/2 phosphorylation and a slight reduction in Akt phosphorylation. Akt, c-jun, and Hsp27 phosphorylation signatures were more sensitive to culture medium conditions regardless of the

presence of the inhibitor. Further, p38 phosphorylation is decreased at day 14 in Exp media but does not in OS medium. Culture on tEGF affects a number of the kinase activation patterns. MSC on control surfaces with OS medium have low levels of phosphorylated ERK compared to those in Exp medium and MSC on tEGF in OS medium at earlier time points, but the OS treatment values converge by day 7.

The severe challenge of interpreting, solely by intuitive inspection, the relationships of magnitude and/or timing of signals to phenotypic outcomes is illustrated in Figure 3. This set of plots show reorganization of the data to indicate whether any clear univariate correlations (i.e., any particular individual signal in isolation) between signals and phenotypic behavior might be apparent. We calculated the integral of the activation using the area under the curve (AUC) for four representative kinase phosphosignals (p-EGFR, p-ERK, p-Akt, p-p38), capturing the magnitude and duration of the activation (rather than comparing the maximal value for specific condition or time point). This metric was chosen because differentiation and proliferation occur over extended time periods, thus integrating over time, effects of signaling pathway activities that may influence outcomes. These plots illustrate the problem in attempting to identify monotonic dependences of phenotypic behavior on any individual signal univariately, as the signal-response relationships are quite complex. In some cases a threshold-like behavior is suggested for which increase of a particular phosphosignal above a certain level is associated with a dramatic change in phenotypic behavior. It is conceivable that some signal-response relationships are more “digital” in nature, with signal levels above or below a threshold value associated with a particular behavior. With all the signals co-varying, however, identifying simple dependences of a phenotypic response on any single signal becomes elusive when a diverse landscape of treatment conditions is considered.

Partial Least-Squares Regression model identifies critical kinase signal combinations predictive for MSC proliferation and osteogenic differentiation

To construct predictive models that relate quantitative combinations of multiple signals to phenotypic outcomes across diverse culture conditions, we used partial least squares regression (PLSR). This computational technique uses linear algebra to reduce the dimensionality of multi-variate data sets by defining principle component (PC) axes from the original data set that contain the most important information. Simca-P is the software package we used to perform the calculations after inputting the normalized and unit scaled data from Figures 1 and 2. PLSR first decomposes multidimensional data into a few PC axes with an algorithm that captures the maximal variance, and thus, the greatest information. The algorithm uses a proposed relationship, defined by the user, between the independent (signals; X) and dependent (responses; Y) variables. The data set is then regressed with a linear solution in principal component space such that $Y=F(X)$. The variables (kinase signals in this case) exhibiting strongest covariance contributing most to the dependent variable outputs (proliferation and differentiation responses here) are weighted more heavily in the solution/prediction function $Y=F(X)$. In essence, the “noise” of the less important signaling variables and times become “muted”, and the important signals and metrics become “loud”; this $Y=F(X)$ function that has now been defined can be used to mathematically predict a response (Y) from the input data matrix (X), and in doing so, reduce the amount of information necessary for an accurate prediction.

The ‘scores plot’ in reduced-dimensions (principal component axes) is a graph of the treatments as the model groups them according to their covariance and projects them onto each PC. The results are shown in Figure 4. MSCs cultured in OS medium are seen to separate along PC 1 from those in Exp medium, and PC 2 separates MSCs on tEGF from those on control surfaces (Fig 4A). Interestingly, MSCs cultured on tEGF and treated with AG1478, are grouped closer to control than their tEGF uninhibited counterparts; the model has done this based solely on

the kinase signatures measured over these time points without specifying external knowledge concerning any particular effects (such as "AG" being an inhibitor of EGFR kinase activity) (Fig 4A). In Figure 4B, the responses of proliferation (21 day cell number) and differentiation (21 day Alizarin Red) are separated along PC 1. Taken together, the first PC can be defined as the osteogenic differentiation vs. proliferation axis and the second PC as the tEGF influence axis (Fig 4C). It can be inferred that tEGF contributes more to osteogenic differentiation (here, 21 day Alizarin Red) than cell number (21 day cell number) by comparing the magnitude (*i.e.*, perpendicular length) of the response vector projections onto PC 2 (Fig 4C); 21 day Alizarin Red is almost three times the perpendicular length from the x-axis than 21 day cell number.

Kinase signals organize toward a phenotypic response by day 7

The 'loadings plot' summarizes the corresponding influence that each signal has on a response, in context of all the other signal effects, represented by the weight it is given in the calculation/prediction function Y=F(X) where Y and X are M × N matrices spanning the time points and kinase signals measured. Mapping the loadings in Figure 5 provides a visual representation of their contribution to the two responses, enabling tracking of the kinase signals with respect to cell fate decision processes over time. Total kinase levels in PC space cluster with cell proliferation at day 4 (green, Supplementary Fig 2), but contribute more to the 21 day OS differentiation response by day 7 (black, Supplementary Fig 2). Interestingly, kinase phosphosite contributions are widely dispersed throughout the PC space at day 4 (Fig 5A). By day 7, however, phosphorylation levels have clearly polarized to osteogenic differentiation or proliferation outcomes (Fig 5B) as judged by their close proximity on the loadings plot in PC space. GSK3α/β either seems to contribute equally to both, or not significantly involved with the responses measured.

New PLSR models were constructed relating each of the signal time-points (i.e., day 4, day 7, or day 14) to day 21 cell responses of proliferation and matrix mineralization, in order to evaluate their respective predictive capabilities. A model was exclusively trained with only day 4, or day 7, or day 14 signals to calculate day 21 responses. Prediction ability was determined using the weights assigned to each kinase in the particularly associated new function Y=F(X), to calculate and predict day 21 values; those predictions were then compared with actual observed values. 100% predictability would mean the calculated values across all treatment conditions would be the same as observed values across all treatment conditions. As shown in Figure 5C, each of the time-points provides kinase signal combinations that are reasonably predictive of the day 21 phenotypic outcomes. Interestingly, the strongest predictive capability is achieved by the day 7 signals. This result implies: [a] that execution of proliferation and differentiation behavior is governed by a quantitative combination of kinase signals across the full set of culture conditions; and [b] that the time-frame for this governance to be manifested (presumably by ensuing gene expression and feedback to the regulatory pathways internally and externally) is on the order of at least a week or two – i.e., the difference between day 21 outcomes and day 7 signals.

Identification of the most important kinase signals reduces the amount of data required to accurately predict MSC responses

Development of this data-driven model required a large number of signaling measurements: ~1060 measurements of 8 kinases, 2 ligands, and 7-day alkaline phosphatase activity, across 8 treatment conditions with at least 7 different assays and up to 5 time points. Along with the predictive modeling capability itself, PLSR analysis also can identify the most important signals for a cellular outcome by calculating the variable importance for projection (VIP) using a weighted sum of squares, such that signals projecting strongly either positively or negatively with a response are highly ranked. In Table 1, we show that the top 7 VIPs, and 12 out of the

top 20, are from day 7 determined by a model trained with our entire data set of vehicle and inhibitor data over 14 days, matched to 21 day response of matrix mineralization. To ease the effort and cost of a 21 day experiment, collection of kinase signals at one relatively early, highly predictive time point would be beneficial; a prime time point is 7 days especially since it also provided the greatest predictability of 21 day outputs when the model is trained with only a single day's input (Fig. 5C).

To facilitate experimental simplification and cost reduction, we limited the model training set to only Novagen and Bioplex assays at day 7, becoming a two lysate-four assay condition, and were able to retain 99% predictability of 21-day matrix mineralization. Even further reduction to a one lysate-two assay condition with only the phosphosites for EGFR, Akt, ERK 1/2, Hsp27, c-jun, GSK3α/β, p38 MAPK, and STAT3 at day 7 retained 93% predictability of 21 day matrix mineralization by MSCs cultured in osteogenic media on control or tEGF surfaces (Supplementary Table 1).

A priori prediction of the combined effects on 21 day OS differentiation and matrix mineralization of tEGF and collagen

To determine whether our reduced model could be used to make *a priori* predictions of MSC differentiation under untested, microenvironmental changes, MSCs were seeded on type I collagen coated polymeric scaffolds with or without tethered EGF and cultured for 7 days. It is known that integrin engagement of extracellular matrix proteins activates intracellular signaling cascades that control cell behavior, and collagen, specifically, has been shown to contribute to the differentiation of MSCs and other pre-osteoblastic cell types[18, 50, 51]. However, it remains uncertain how signals downstream of integrins and growth factor receptors are quantitatively integrated to corporately regulate phenotypic behavior. We chose to test two hypotheses with our model: first, if collection of only 7 day kinase phosphorylation signals would be predictive of the 21 day mineralization of MSCs on type I collagen; and second, if there is a synergistic effect between tEGF and collagen on increasing MSC osteogenic differentiation and matrix mineralization. The results are shown in Figure 6.

To generate a new and independent experimental data-set for direct test of PLSR model predictions corresponding to these hypotheses, surfaces were prepared as previously except that 1 μg/ml of type I collagen was adsorbed at room temperature for one hour prior to cell seeding. After 24 hours, medium was changed to OS and changed every third day. On day 7, samples were collected, total protein determined, and phosphorylation was determined as above. Phase images of the cells on the different surfaces at day 7 are shown (Fig. 6A). The profiles of the measured kinase phosphorylation signals differ between the collagen coated surfaces and the no ECM controls (Fig 6B). These newly-generated day 7 phosphosite measurements were inserted into the PLSR model originally constructed from the earlier data-set, and weighted coefficients were mathematically determined according to the NIPALS algorithm as described above for the full data set. Simca-P algorithms then calculated phenotypic outcomes (scaled between 0 and 1) for 21-day matrix mineralization, and the predicted control (no ECM) responses matched previously observed 21-day matrix mineralization results where tEGF caused a two-fold increase over control. On control, uncoated surfaces without tEGF, the model predicted that type I collagen would increase matrix mineralization. However, it predicted that the combination of type I collagen and tEGF would reduce the 21-day matrix mineralization from that of just tEGF, not enhance it (Fig 6C).

To test this result experimentally, MSCs were seeded, cultured for 21 days, fixed, stained with Alizarin Red S, imaged, and quantified as above. These results successfully realized the model predictions: on control surfaces coated with type I collagen, MSCs created more mineralized matrix than the matching no-ECM controls, and the synergy of tEGF and collagen reduced matrix mineralization from that of tEGF alone (Fig 6D). More importantly, this result verified

that collection of 7-day kinase signatures were predictive of 21-day mineralization of MSCs under different conditions using our computational model developed with partial least squares regression.

DISCUSSION

MSCs have been proposed in tissue engineering to regenerate bone. However, early attempts have been stymied by both low numbers of MSCs and the death of these cells when implanted in vivo. Recently we reported that MSCs can be expanded ex vivo by EGF, and that EGF, when presented in a tethered manner, protects these cells from death[7,8]. This led to the finding that culturing MSCs on tethered EGF enhances the osteoinductive properties of osteogenic stimuli via sustained EGFR phosphorylation[10], offering a new biomaterials-oriented approach to enhancing osteogenic differentiation. However, it was not evident whether this arose from greater activity per cell or augmented number of surviving MSCs, or both. Thus we sought to enhance this approach by means of additional growth factors, extracellular matrix adhesion ligands, and/or small molecule pathway modulators. However, rational usage of multiple cues requires increased understanding of their signaling pathway activation to regulate phenotypic behavior[52, 53]. For regulation of embryonic stem cell self-renewal and differentiation[54] as well as a spectrum of other cell fate decisions[55–59], individual signaling pathways are not univariately predictive of responses to extracellular stimuli nor are input cues simply additive or even synergistic; instead, rational prediction of cell fate outcomes across diverse treatment conditions requires determination of how multiple pathways are quantitatively combined into a ‘network state’ that integratively governs response. We apply this approach here to gain predictive understanding of MSC osteogenic differentiation in response to different biomaterials culture conditions, including tethered EGF in presence or absence of collagen-I.

For the foundational study of MSCs cultured on tEGF versus control substrata (and +/− an EGFR inhibitor), Figure 2 shows the time-courses of measured signal phosphosites: p-EGFR, p-ERK1/2, p-Akt, p-p38, p-HSP27, p-c-Jun, p-STAT3, and p-GSK3α/β. Figure 3 illustrates that none of these signals are strongly correlated with cell proliferation or differentiation outcomes across all culture conditions. In contrast, Figure 5C shows that a computational model using partial least-squares regression ascertains quantitatively weighted combinations of these signal phosphosites capable of predicting osteogenic differentiation behavior across these culture conditions, and Figure 5B locates the qualitative and quantitative contributions of the various signals to the model: p-EGFR, p-Akt, and p-HSP27 are found strongly positively associated with mineralization activity while p-ERK is found strongly negatively associated; p-p38 contributes mildly in positive manner whereas p-c-jun contributes mildly in negative manner.

We then proceeded to test this predictive model capability for its utility in understanding the effects of culture on type I collagen, a major structural protein of bone and produced during osteogenic differentiation. Bone progenitor cells lay down collagen prior to matrix mineralization[60, 61] and most likely do so on our polymer surfaces whether EGF is tethered or not. The ultimate goal is to use this material for clinical bone grafts to be seeded with a patient’s own bone marrow progenitor cells, and coating these surfaces with matrix proteins preferred by the cells is an attractive method for enhancing desired MSC behavior. This was not the case with collagen I, however. It did increase MSC osteogenic differentiation with no tEGF (Fig 6D) as has been reported[62–64], but MSC engagement of EGFR with tEGF and integrin binding to collagen I actually mitigated the differentiation response induced by tEGF alone (Fig 6C, D). Reports have shown that soluble EGF decreases collagen I synthesis[30] but the converse has not been shown. Figure 6C shows the integrated effects of the growth factor and extracellular matrix ligands on the kinase signaling network activities and that our PLSR model comprehends all these effects. It successfully predicted, in a completely *a priori* manner,

osteogenic differentiation under a new, independent set of culture conditions involving substrate coated with collagen-I in presence or absence of tEGF. The effects of this materials-based outcome could not be obviously anticipated, for as shown in Figure 6B the influence of collagen-I on the various kinase signals is quite diverse rendering prediction of consequent phenotypic effects difficult.

The kinase signals chosen for this study are generally appreciated to serve as major integrators of disparate canonical pathways. Kinase phosphorylation is transient due to the dynamic interplay between kinases and phosphatases. It may at first glance seem somewhat surprising that transient tools used by cells to transduce extracellular information would be able to predict phenotypic behavior a week or more later, as is demonstrated in Figure 5C. However, upon reflection it is realized (as illustrated in Figure 7A) that signaling network activities at a given point in time lead to alterations in gene expression (as well as metabolic and cytoskeletal processes) that ultimately execute observable phenotypic behavior, or metaphorically, resets the keyboard upon which the subsequent song is played. Along the way, the signaling network is modulated further by feedback from alterations in gene expression that operate both intracellularly and extracellularly. An intriguing question associated with this understanding is what the time-frame containing the most informative network signaling measurements might be. Figure 7B illustrates this conceptually for the day-21 differentiation outcome studied in this present work. Network activity at an intermediate time-point might be most informative due to a temporal balance between fate decision and effector actions; the earliest time-points may be less informative because more uncertainty exists concerning the evolution of the gene expression-related feedback loops, and the latest time-points may be less informative because the cell fate decision is largely determined before all the ensuing processes are completely played out. Figure 5C shows the actual result of our combined experimental/computational study, with day-7 network activity being most informative for prediction of day-21 phenotype. Nonetheless, it is not the case that day 7 is a “lucky guess” or “magic window” because Figure 5C also shows that day-4 and day-14 signals are also at least reasonably effective in the day-21 outcome prediction. Interestingly, a previous study of a different cell phenotypic fate decision – apoptotic cell death – similarly found that maximal predictive capability of signaling network information was obtained within an intermediate time-frame[65].

As MSCs differentiate into osteoprogenitors and osteoblasts, timed activation and inactivation of histone acetylases and deacetylases, transcription factors, extracellular matrix production, and osteoblast-specific enzymatic activity are regulated by signals intra- and extra-cellularly as well as intra- and extra-nuclearly; Runx2, TGF-β, Wnt, and osteopontin along with collagen I being among the most intensely studied. Reviews of these interactions and feedback/feed-forward loops have highlighted important findings identifying contributions of various components and pathways during periods of MSC proliferation, maturation, and matrix mineralization[60, 66–70]. We note here the timing of peaks of maximal mRNA expression of collagen I and alkaline phosphatase (early and mid) compared to osteocalcin and collagenase (late)[66] represents transcriptional processes preparing for the next phase of differentiation, supporting our Figure 7 schematic that potentially explains our finding that day 7 kinase signals are more predictive than day 14 signals for day 21 mineralization. Absent intervening perturbations, our results are consistent with gene expression literature on chronological programming of differentiation from extracellular cues to signaling activities to gene expression, with feedback loops at both extracellular and intracellular aspects of the regulatory process.

This study highlights more than the particular pattern of signal-response relationships for this focused cell culture study. It is quite plausible that assessment of a comparable though alternatively specified set of signaling network nodes could produce a similarly predictive model for longer-term osteogenesis. Such a model enabling prediction of cell fate outcomes

from a dynamic network signature could perhaps be utilized for more deeply informative testing combinations of cues (materials, growth factors, extracellular matrix, and/or small molecules), permitting increased effectiveness in translation between *ex vivo* and in vivo outcomes by means of the multi-variate signal-response model relationships[74].

Supplementary Material

Refer to Web version on PubMed Central for supplementary material.

Acknowledgments

The authors are grateful to Linda Stockdale, Arthur Goldsipe, and Benjamin Cosgrove for technical assistance, for funding provided by NIH R01-GM059870-07 (LGG), R01 DE019523-10 (LGG and AW), NIH R01-GM69668 (AW and DAL), UNCF/Merck Postdoctoral Fellowship (MOP), and Georgia Tech FACES Fellowship (MOP). Some of the materials employed were provided by the Tulane Center for Gene Therapy through NCRR grant P40RR017447.

REFERENCES

1. Friedenstein AJ, Piatetzky S II, Petrakova KV. Osteogenesis in transplants of bone marrow cells. J Embryol Exp Morphol 1966;16:381–390. [PubMed: 5336210]
2. Pittenger MF, Mackay AM, Beck SC, et al. Multilineage potential of adult human mesenchymal stem cells. Science 1999;284:143–147. [PubMed: 10102814]
3. Sekiya I, Larson BL, Smith JR, et al. Expansion of human adult stem cells from bone marrow stroma: conditions that maximize the yields of early progenitors and evaluate their quality. Stem Cells 2002;20:530–541. [PubMed: 12456961]
4. Krampera M, Pasini A, Rigo A, et al. HB-EGF/HER-1 signaling in bone marrow mesenchymal stem cells: inducing cell expansion and reversibly preventing multilineage differentiation. Blood 2005;106:59–66. [PubMed: 15755902]
5. Kratchmarova I, Blagoev B, Haack-Sorensen M, et al. Mechanism of divergent growth factor effects in mesenchymal stem cell differentiation. Science 2005;308:1472–1477. [PubMed: 15933201]
6. Sibilia M, Wagner B, Hoebertz A, et al. Mice humanised for the EGF receptor display hypomorphic phenotypes in skin, bone and heart. Development 2003;130:4515–4525. [PubMed: 12925580]
7. Tamama K, Fan VH, Griffith LG, et al. Epidermal growth factor as a candidate for ex vivo expansion of bone marrow-derived mesenchymal stem cells. Stem Cells 2006;24:686–695. [PubMed: 16150920]
8. Fan VH, Tamama K, Au A, et al. Tethered epidermal growth factor provides a survival advantage to mesenchymal stem cells. Stem Cells 2007;25:1241–1251. [PubMed: 17234993]
9. Kuhl PR, Griffith-Cima LG. Tethered epidermal growth factor as a paradigm for growth factor-induced stimulation from the solid phase. Nat Med 1996;2:1022–1027. [PubMed: 8782461]
10. Platt MO, Roman AJ, Wells A, et al. Sustained epidermal growth factor receptor levels and activation by tethered ligand binding enhances osteogenic differentiation of multi-potent marrow stromal cells. J Cell Physiol. 2009
11. Ge C, Xiao G, Jiang D, et al. Critical role of the extracellular signal-regulated kinase-MAPK pathway in osteoblast differentiation and skeletal development. J Cell Biol 2007;176:709–718. [PubMed: 17325210]
12. Higuchi C, Myoui A, Hashimoto N, et al. Continuous inhibition of MAPK signaling promotes the early osteoblastic differentiation and mineralization of the extracellular matrix. J Bone Miner Res 2002;17:1785–1794. [PubMed: 12369782]
13. Jaiswal RK, Jaiswal N, Bruder SP, et al. Adult human mesenchymal stem cell differentiation to the osteogenic or adipogenic lineage is regulated by mitogen-activated protein kinase. J Biol Chem 2000;275:9645–9652. [PubMed: 10734116]
14. Watton SJ, Downward J. Akt/PKB localisation and 3' phosphoinositide generation at sites of epithelial cell-matrix and cell-cell interaction. Curr Biol 1999;9:433–436. [PubMed: 10226029]

15. Wu CJ, Chen Z, Ullrich A, et al. Inhibition of EGFR-mediated phosphoinositide-3-OH kinase (PI3-K) signaling and glioblastoma phenotype by signal-regulatory proteins (SIRPs). Oncogene 2000;19:3999–4010. [PubMed: 10962556]

16. Fujita T, Azuma Y, Fukuyama R, et al. Runx2 induces osteoblast and chondrocyte differentiation and enhances their migration by coupling with PI3K-Akt signaling. J Cell Biol 2004;166:85–95. [PubMed: 15226309]

17. Kawamura N, Kugimiya F, Oshima Y, et al. Akt1 in osteoblasts and osteoclasts controls bone remodeling. PLoS ONE 2007;2:e1058. [PubMed: 17957242]

18. Kundu AK, Khatiwala CB, Putnam AJ. Extracellular Matrix Remodeling, Integrin Expression, and Downstream Signaling Pathways Influence the Osteogenic Differentiation of Mesenchymal Stem Cells on Poly(Lactide-Co-Glycolide) Substrates. Tissue Eng Part A. 2008

19. Osyczka AM, Leboy PS. Bone morphogenetic protein regulation of early osteoblast genes in human marrow stromal cells is mediated by extracellular signal-regulated kinase and phosphatidylinositol 3-kinase signaling. Endocrinology 2005;146:3428–3437. [PubMed: 15905316]

20. Baksh D, Tuan RS. Canonical and non-canonical Wnts differentially affect the development potential of primary isolate of human bone marrow mesenchymal stem cells. J Cell Physiol 2007;212:817–826. [PubMed: 17458904]

21. Boland GM, Perkins G, Hall DJ, et al. Wnt 3a promotes proliferation and suppresses osteogenic differentiation of adult human mesenchymal stem cells. J Cell Biochem 2004;93:1210–1230. [PubMed: 15486964]

22. Caverzasio J, Manen D. Essential role of Wnt3a-mediated activation of mitogen-activated protein kinase p38 for the stimulation of alkaline phosphatase activity and matrix mineralization in C3H10T1/2 mesenchymal cells. Endocrinology 2007;148:5323–5330. [PubMed: 17717053]

23. Chang J, Sonoyama W, Wang Z, et al. Noncanonical Wnt-4 signaling enhances bone regeneration of mesenchymal stem cells in craniofacial defects through activation of p38 MAPK. J Biol Chem 2007;282:30938–30948. [PubMed: 17720811]

24. Chen YJ, Kuo YR, Yang KD, et al. Activation of extracellular signal-regulated kinase (ERK) and p38 kinase in shock wave-promoted bone formation of segmental defect in rats. Bone 2004;34:466–477. [PubMed: 15003794]

25. Kugimiya F, Kawaguchi H, Ohba S, et al. GSK-3beta controls osteogenesis through regulating Runx2 activity. PLoS ONE 2007;2:e837. [PubMed: 17786208]

26. Janes KA, Albeck JG, Gaudet S, et al. A systems model of signaling identifies a molecular basis set for cytokine-induced apoptosis. Science 2005;310:1646–1653. [PubMed: 16339439]

27. Miller-Jensen K, Janes KA, Brugge JS, et al. Common effector processing mediates cell-specific responses to stimuli. Nature 2007;448:604–608. [PubMed: 17637676]

28. Gronthos S, Simmons PJ. The growth factor requirements of STRO-1-positive human bone marrow stromal precursors under serum-deprived conditions in vitro. Blood 1995;85:929–940. [PubMed: 7849315]

29. Harrington M, Pond-Tor S, Boney CM. Role of epidermal growth factor and ErbB2 receptors in 3T3-L1 adipogenesis. Obesity 2007;15:563–571. [PubMed: 17372305]

30. Kumegawa M, Hiramatsu M, Hatakeyama K, et al. Effects of epidermal growth factor on osteoblastic cells in vitro. Calcif Tissue Int 1983;35:542–548. [PubMed: 6604567]

31. Sato H, Kuwashima N, Sakaida T, et al. Epidermal growth factor receptor-transfected bone marrow stromal cells exhibit enhanced migratory response and therapeutic potential against murine brain tumors. Cancer Gene Ther 2005;12:757–768. [PubMed: 15832173]

32. Zhu J, Jia X, Xiao G, et al. EGF-like ligands stimulate osteoclastogenesis by regulating expression of osteoclast regulatory factors by osteoblasts: implications for osteolytic bone metastases. J Biol Chem 2007;282:26656–26664. [PubMed: 17636266]

33. Hong JH, Hwang ES, McManus MT, et al. TAZ, a transcriptional modulator of mesenchymal stem cell differentiation. Science 2005;309:1074–1078. [PubMed: 16099986]

34. Kanno T, Takahashi T, Tsujisawa T, et al. Mechanical stress-mediated Runx2 activation is dependent on Ras/ERK1/2 MAPK signaling in osteoblasts. J Cell Biochem 2007;101:1266–1277. [PubMed: 17265428]

35. Klees RF, Salasznyk RM, Kingsley K, et al. Laminin-5 induces osteogenic gene expression in human mesenchymal stem cells through an ERK-dependent pathway. Mol Biol Cell 2005;16:881–890. [PubMed: 15574877]
36. Salasznyk RM, Klees RF, Williams WA, et al. Focal adhesion kinase signaling pathways regulate the osteogenic differentiation of human mesenchymal stem cells. Exp Cell Res 2007;313:22–37. [PubMed: 17081517]
37. Sowa H, Kaji H, Yamaguchi T, et al. Activations of ERK1/2 and JNK by transforming growth factor beta negatively regulate Smad3-induced alkaline phosphatase activity and mineralization in mouse osteoblastic cells. J Biol Chem 2002;277:36024–36031. [PubMed: 12130649]
38. Cheng XW, Kuzuya M, Sasaki T, et al. Increased expression of elastolytic cysteine proteases, cathepsins S and K, in the neointima of balloon-injured rat carotid arteries. Am J Pathol 2004;164:243–251. [PubMed: 14695337]
39. Lee HW, Suh JH, Kim HN, et al. Berberine promotes osteoblast differentiation by Runx2 activation with p38 MAPK. J Bone Miner Res 2008;23:1227–1237. [PubMed: 18410224]
40. McMahon LA, Prendergast PJ, Campbell VA. A comparison of the involvement of p38, ERK1/2 and PI3K in growth factor-induced chondrogenic differentiation of mesenchymal stem cells. Biochem Biophys Res Commun 2008;368:990–995. [PubMed: 18267113]
41. Simmons CA, Matlis S, Thornton AJ, et al. Cyclic strain enhances matrix mineralization by adult human mesenchymal stem cells via the extracellular signal-regulated kinase (ERK1/2) signaling pathway. J Biomech 2003;36:1087–1096. [PubMed: 12831733]
42. Leonardi R, Barbato E, Paganelli C, et al. Immunolocalization of heat shock protein 27 in developing jaw bones and tooth germs of human fetuses. Calcif Tissue Int 2004;75:509–516. [PubMed: 15654495]
43. McCabe LR, Banerjee C, Kundu R, et al. Developmental expression and activities of specific fos and jun proteins are functionally related to osteoblast maturation: role of Fra-2 and Jun D during differentiation. Endocrinology 1996;137:4398–4408. [PubMed: 8828501]
44. Winchester SK, Selvamurugan N, D'Alonzo RC, et al. Developmental regulation of collagenase-3 mRNA in normal, differentiating osteoblasts through the activator protein-1 and the runt domain binding sites. J Biol Chem 2000;275:23310–23318. [PubMed: 10779518]
45. Zayzafoon M, Stell C, Irwin R, et al. Extracellular glucose influences osteoblast differentiation and c-Jun expression. J Cell Biochem 2000;79:301–310. [PubMed: 10967557]
46. Wang M, Zhang W, Crisostomo P, et al. STAT3 mediates bone marrow mesenchymal stem cell VEGF production. J Mol Cell Cardiol 2007;42:1009–1015. [PubMed: 17509611]
47. Baksh D, Boland GM, Tuan RS. Cross-talk between Wnt signaling pathways in human mesenchymal stem cells leads to functional antagonism during osteogenic differentiation. J Cell Biochem 2007;101:1109–1124. [PubMed: 17546602]
48. Gaur T, Lengner CJ, Hovhannisyan H, et al. Canonical WNT signaling promotes osteogenesis by directly stimulating Runx2 gene expression. J Biol Chem 2005;280:33132–33140. [PubMed: 16043491]
49. Kumar N, Wolf-Yadlin A, White FM, et al. Modeling HER2 effects on cell behavior from mass spectrometry phosphotyrosine data. PLoS Comput Biol 2007;3:e4. [PubMed: 17206861]
50. Cool SM, Nurcombe V. Substrate induction of osteogenesis from marrow-derived mesenchymal precursors. Stem Cells Dev 2005;14:632–642. [PubMed: 16433618]
51. Salasznyk RM, Williams WA, Boskey A, et al. Adhesion to Vitronectin and Collagen I Promotes Osteogenic Differentiation of Human Mesenchymal Stem Cells. J Biomed Biotechnol 2004;2004:24–34. [PubMed: 15123885]
52. Caplan MR, Shah MM. Translating biomaterial properties to intracellular signaling. Cell Biochem Biophys 2009;54:1–10. [PubMed: 19390790]
53. Ding S, Schultz PG. Small molecules and future regenerative medicine. Curr Top Med Chem 2005;5:383–395. [PubMed: 15892681]
54. Prudhomme W, Daley GQ, Zandstra P, et al. Multivariate proteomic analysis of murine embryonic stem cell self-renewal versus differentiation signaling. Proc Natl Acad Sci U S A 2004;101:2900–2905. [PubMed: 14978270]

55. Citri A, Skaria KB, Yarden Y. The deaf and the dumb: the biology of ErbB-2 and ErbB-3. Exp Cell Res 2003;284:54–65. [PubMed: 12648465]
56. Wiley HS. Trafficking of the ErbB receptors and its influence on signaling. Exp Cell Res 2003;284:78–88. [PubMed: 12648467]
57. Breuleux M. Role of heregulin in human cancer. Cell Mol Life Sci 2007;64:2358–2377. [PubMed: 17530167]
58. Yarden Y, Shilo BZ. SnapShot: EGFR signaling pathway. Cell 2007;131:1018. [PubMed: 18045542]
59. Kemp ML, Wille L, Lewis CL, et al. Quantitative network signal combinations downstream of TCR activation can predict IL-2 production response. J Immunol 2007;178:4984–4992. [PubMed: 17404280]
60. Franceschi RT. The developmental control of osteoblast-specific gene expression: role of specific transcription factors and the extracellular matrix environment. Crit Rev Oral Biol Med 1999;10:40–57. [PubMed: 10759426]
61. Quarles LD, Yohay DA, Lever LW, et al. Distinct proliferative and differentiated stages of murine MC3T3-E1 cells in culture: an in vitro model of osteoblast development. J Bone Miner Res 1992;7:683–692. [PubMed: 1414487]
62. Andrianarivo AG, Robinson JA, Mann KG, et al. Growth on type I collagen promotes expression of the osteoblastic phenotype in human osteosarcoma MG-63 cells. J Cell Physiol 1992;153:256–265. [PubMed: 1429847]
63. Franceschi RT, Iyer BS. Relationship between collagen synthesis and expression of the osteoblast phenotype in MC3T3-E1 cells. J Bone Miner Res 1992;7:235–246. [PubMed: 1373931]
64. Kundu AK, Putnam AJ. Vitronectin and collagen I differentially regulate osteogenesis in mesenchymal stem cells. Biochem Biophys Res Commun 2006;347:347–357. [PubMed: 16815299]
65. Janes KA, Gaudet S, Albeck JG, et al. The response of human epithelial cells to TNF involves an inducible autocrine cascade. Cell 2006;124:1225–1239. [PubMed: 16564013]
66. Stein GS, Lian JB, Stein JL, et al. Transcriptional control of osteoblast growth and differentiation. Physiol Rev 1996;76:593–629. [PubMed: 8618964]
67. Huang W, Yang S, Shao J, et al. Signaling and transcriptional regulation in osteoblast commitment and differentiation. Front Biosci 2007;12:3068–3092. [PubMed: 17485283]
68. Benayahu D, Shefer G, Shur I. Insights into the transcriptional and chromatin regulation of mesenchymal stem cells in musculo-skeletal tissues. Ann Anat 2009;191:2–12. [PubMed: 18926677]
69. Lian JB, Stein GS, Javed A, et al. Networks and hubs for the transcriptional control of osteoblastogenesis. Rev Endocr Metab Disord 2006;7:1–16. [PubMed: 17051438]
70. Nishimura R, Hata K, Ikeda F, et al. Signal transduction and transcriptional regulation during mesenchymal cell differentiation. J Bone Miner Metab 2008;26:203–212. [PubMed: 18470659]
71. Geladi P. Partial least squares regression: A tutorial. Analytica Chimica Acta 1986;185:1–17.
72. Morita S, Shirakata Y, Shiraishi A, et al. Human corneal epithelial cell proliferation by epiregulin and its cross-induction by other EGF family members. Mol Vis 2007;13:2119–2128. [PubMed: 18079685]
73. Xia Z, Locklin RM, Triffitt JT. Fates and osteogenic differentiation potential of human mesenchymal stem cells in immunocompromised mice. Eur J Cell Biol 2008;87:353–364. [PubMed: 18417247]
74. Cosgrove BD, Griffith LG, Lauffenburger DA. Fusing tissue engineering and systems biology toward fulfilling their promise. Cell Molec Bioeng 2008;1:33–41.

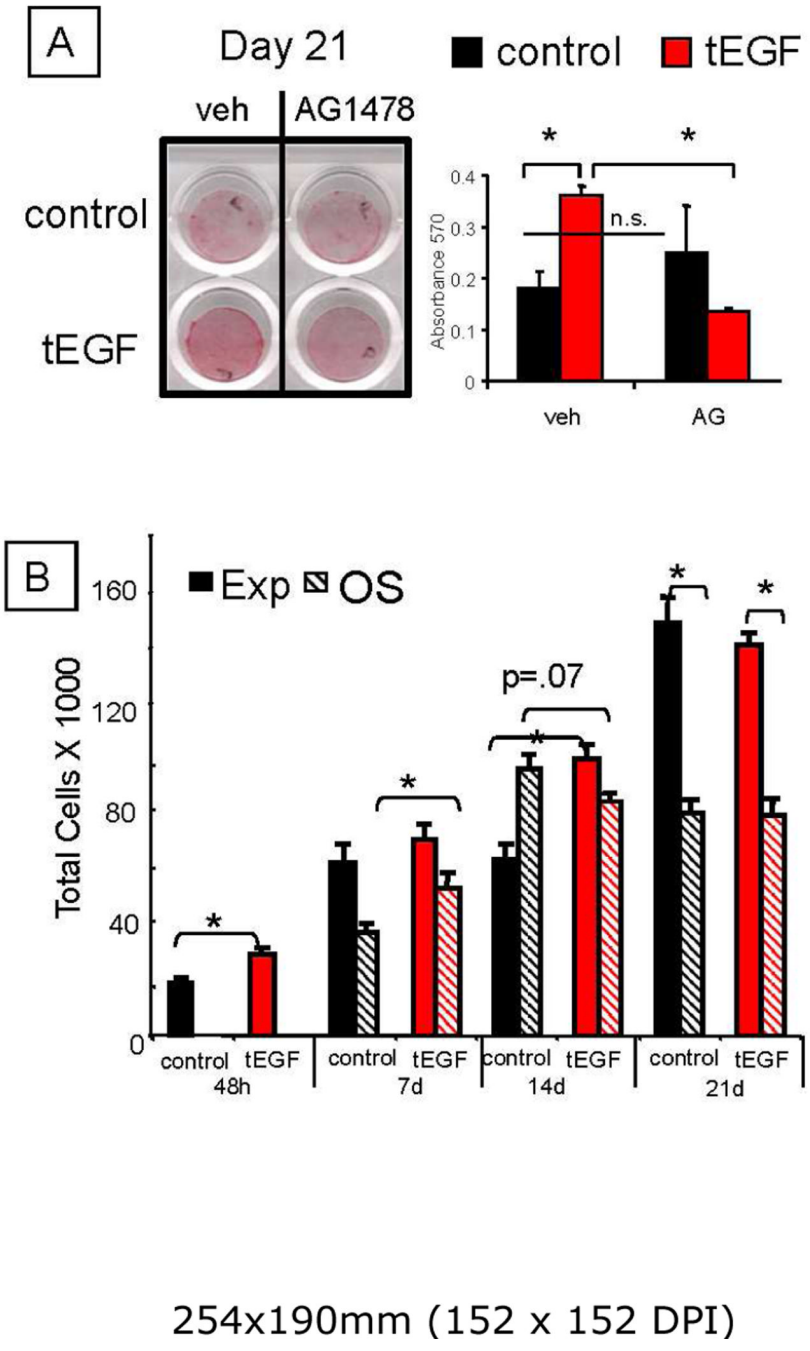

254x190mm (152 x 152 DPI)

Figure 1. Proliferation and differentiation are divergent outcomes for MSCs cultured in the presence of osteoinductive supplements

(A) After 21 days, MSCs were cultured on control or tEGF surfaces for 21 days in osteogenic media in the presence or absence of 1 uM AG1478, then stained with Alizarin Red. Images were captured and quantified (*p<.01, n=3 compared to tEGF vehicle). The result shown is from one representative experiment with n=6, from Reference [10]. **(B)** Human primary MSCs were cultured on control surfaces or on tethered EGF surfaces in expansion (Exp) medium or osteogenic (OS) differentiating media for 2, 4, 7, 14, and 21 days and prepared according to CyQuant protocols. Cell number was calculated by fitting the fluorescence to a standard curve prepared with known cell numbers from a trypsinized plate of MSCs.

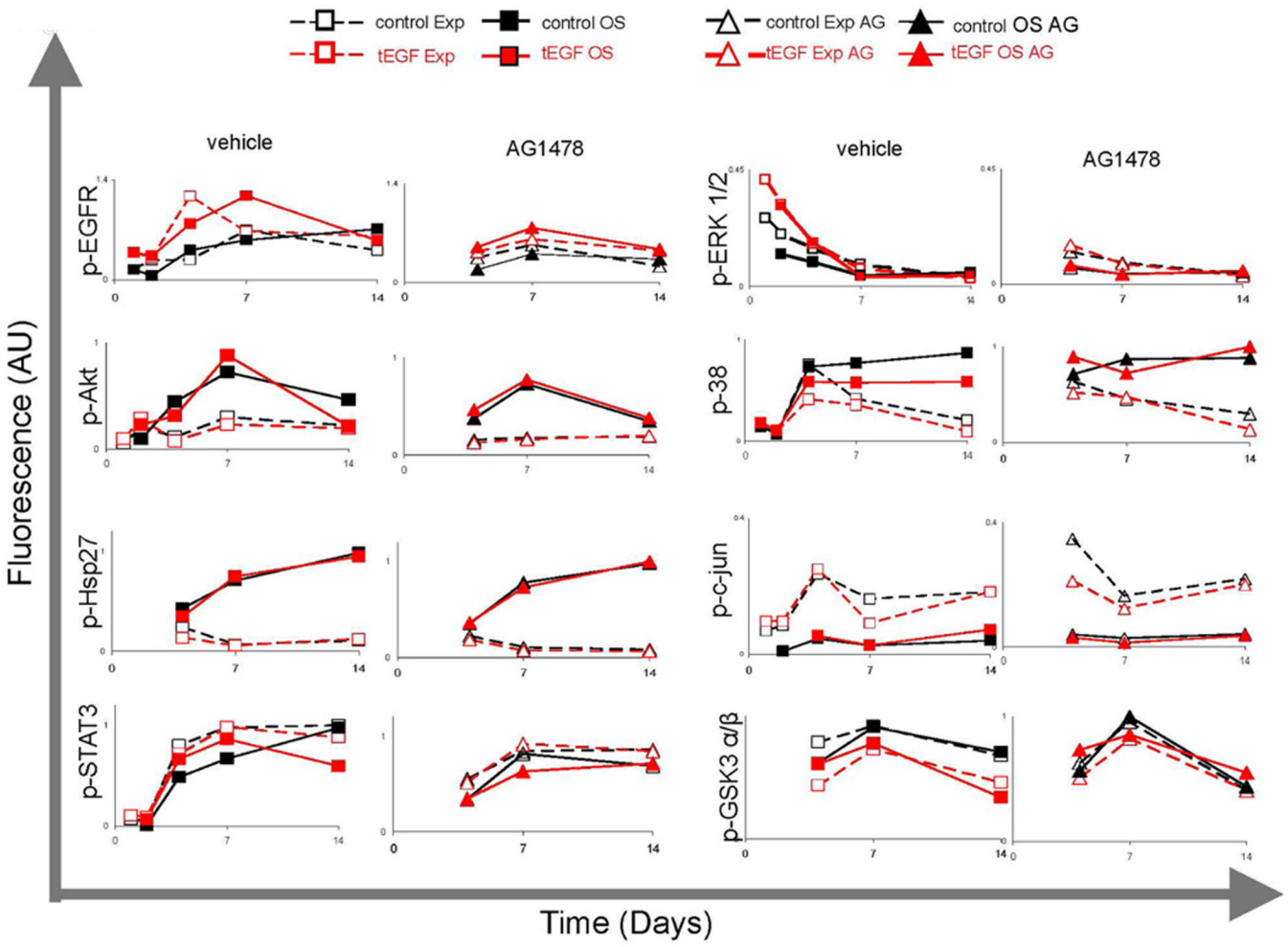

254x190mm (200 x 200 DPI)

Figure 2. Kinase signal collection of time dependent changes during osteogenic differentiation

Human primary MSCs were seeded onto control or tEGF surfaces in Exp medium, then changed to OS or fresh Exp in the presence or absence of 1 μM AG1478, an EGFR kinase inhibitor, for 1, 2, 4, 7, or 14 days followed by cell lysis. Total protein was determined, and equal amounts were loaded for Bioplex or Novagen bead-based immunoprecipitation assays to detect phosphorylation or total protein amounts of the kinases listed. Fluorescence values were normalized to a master lysate and then to the maximum value for each signal to scale the values between 0 and 1. MSC kinase signals data are plotted over 14 days comparing control (black) and tEGF (red) surfaces in Exp (open, dashed line) or OS (closed, solid line) in the absence (squares) or presence (triangles) of 1μM AG1478. Each data point represents the mean of 3–6 biological replicates.

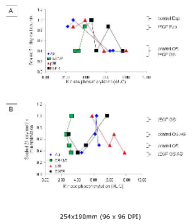

Figure 3. Univariate approaches to analyzing multi-pathway data sets do not fully appreciate the interconnectedness of the signaling networks involved in MSC differentiation and proliferation

Areas under the curve of kinase phosphorylation were calculated for ERK1/2, EGFR, Akt, and p38 MAPK over the 4–14 day period, and plotted on the X-axis with 21-day cell count **(A)** or 21 day matrix mineralization **(B)** or on the Y-axis, for four different treatment conditions in each case. Lines connecting data points are provided as eye-guides to aid the reader in discerning possible trends or lack thereof for the phenotypic responses with respect to the various individual phosphosignals.

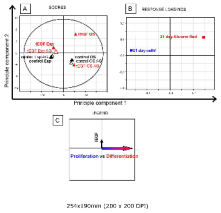

Figure 4. Treatment conditions are successfully separated by a partial least squares regression model trained with kinase signaling dynamics

(A) Treatment conditions are separated by the model in the scores plot, and the EGFR inhibitor on tEGF kinase signals clusters these treatments with control conditions. **(B)** Loadings (weight coefficients) of the two responses are separated along the first principle component. **(C)** Based on the response loadings, the first two PC axes can be defined as 1) proliferation vs. differentiation and 2) tEGF influence.

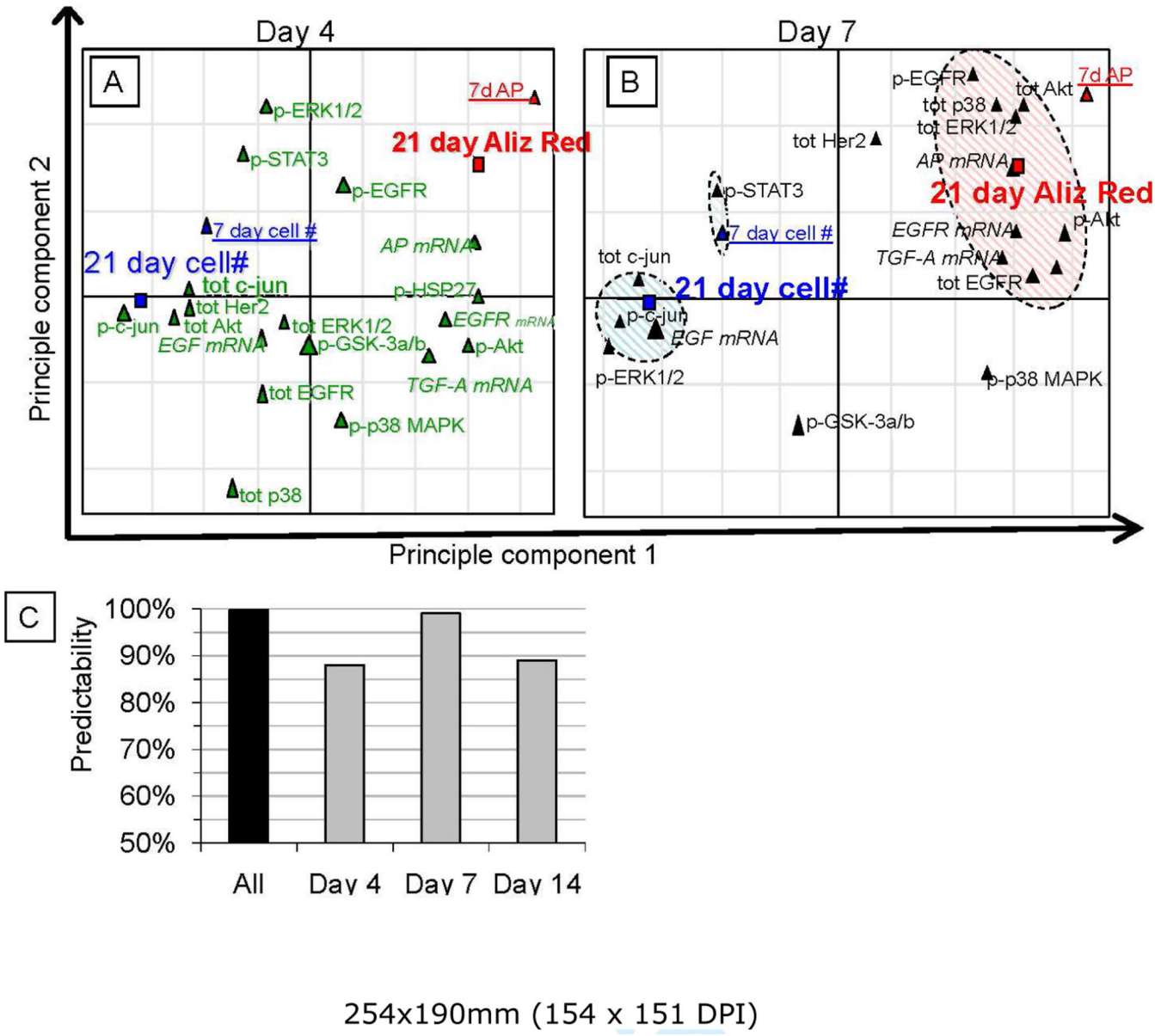

254x190mm (154 x 151 DPI)

Figure 5. Treatment conditions are successfully separated by a partial least squares regression model trained with kinase signaling dynamics

(A) This plot exhibits the loadings of the phosphorylation of each measured kinase at day 4 and their broad distribution whereas by day 7, **(B)** the signals cluster with either the proliferation response (c-jun, ERK, STAT3) or the differentiation response (EGFR, Akt, Hsp27, p38). **(C)** A new model was trained with all signals, or only single day 4, 7, and 14 signals, and predictability for 21-day differentiation were calculated. Predictability was greatest for day 7.

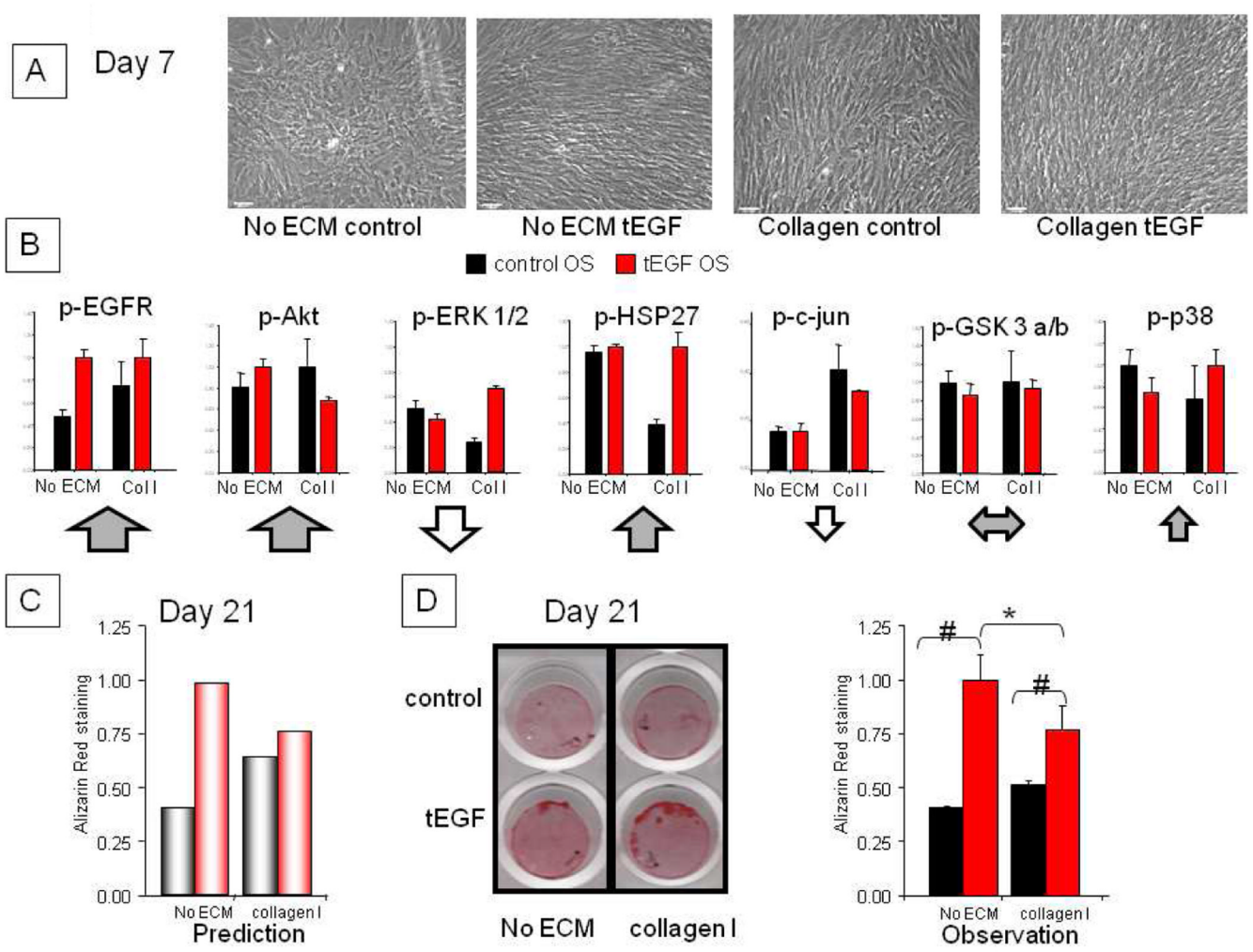

254x190mm (96 x 96 DPI)

Figure 6. Minimal kinase signaling measurements at day 7 predict, *a priori,* the synergistic effects of collagen and tEGF on 21-day matrix mineralization

(A) Phase images under 10X objective of MSCs after 7 days of culture on control or tEGF surfaces preadsorbed with collagen or no ECM control. **(B)**Lysates were collected after 7 days of culture in OS medium on control or tEGF surfaces with or without 1 μg/ml type I collagen, and phosphorylation was determined with Bioplex assays.Arrows underneath each kinase graph are symbolic of each kinase VIP (larger arrows have greater VIPs than smaller arrows: up arrows indicate that phosphorylation of the kinase correlated with promoting OS differentiation, and down arrows correlated with increased cell number and not OS differentiation as determined from the PLSR model. **(C)** Using only these inputs, the model predicted an increase in mineralization on control surfaces in the presence of collagen I, but a decrease in mineralization on both tEGF and collagen I. **(D)** Human primary MSCs were cultured on control or tEGF surfaces for 21 days in osteogenic media with or without 1 μg/ml type I collagen preadsorbed onto the surfaces, then stained with Alizarin Red and quantified. Observations match the model predictions (n=3, *p<.05, #p<.01; p=.06 for control no ECM compared to control collagen I).

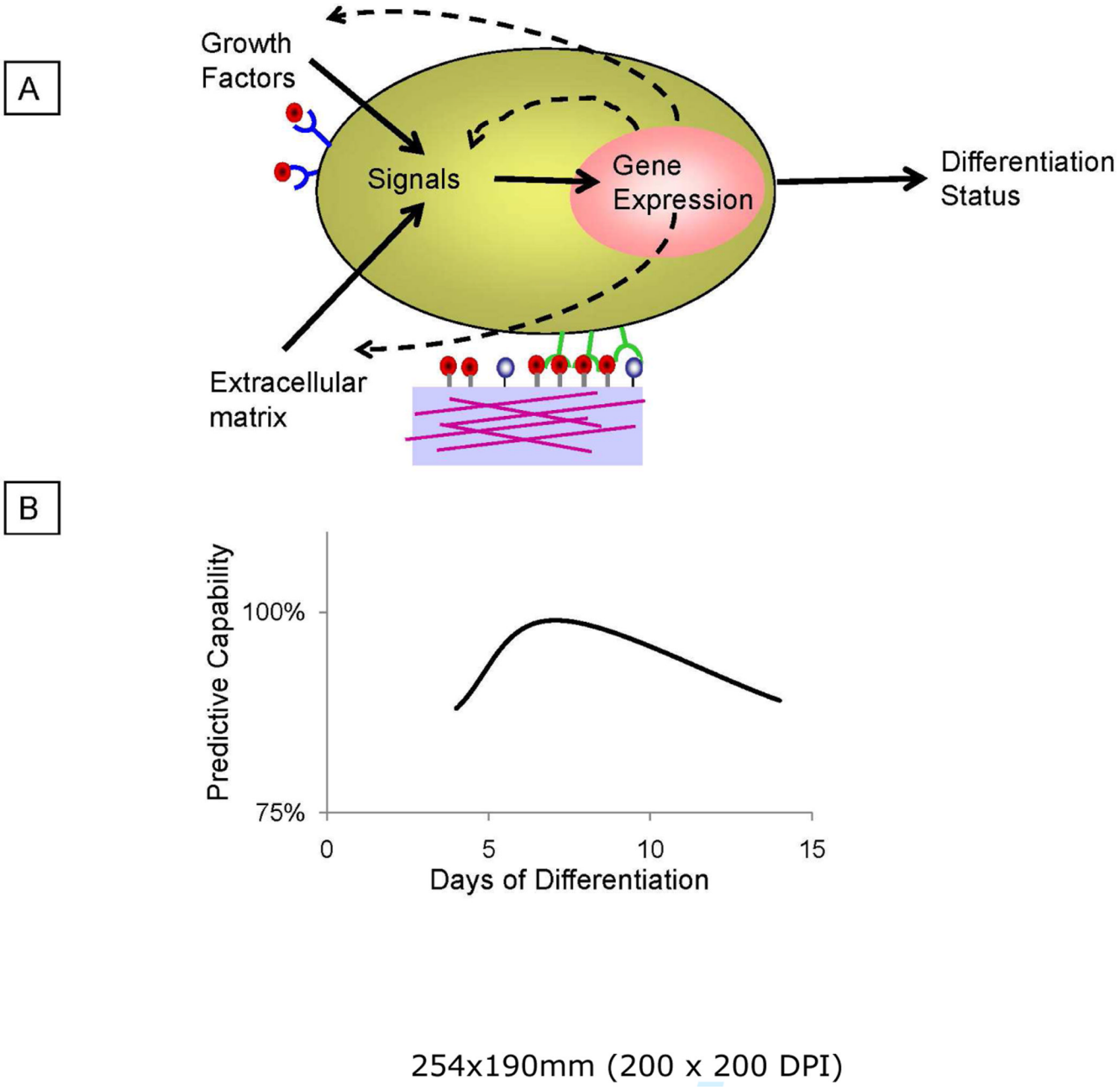

254x190mm (200 x 200 DPI)

Figure 7. Minimal kinase signaling measurements at day 7 predict, *a priori*, the synergistic effects of collagen and tEGF on 21-day matrix mineralization

(A) Schematic diagram of conclusions. Growth factors and extracellular matrix influence kinase activity and gene expression of MSCs. The gene expression and subsequent activities of the MSCs further modify the extracellular matrix and growth factors of the environment as they differentiate which all affect the differentiation status of the cells. **(B)** Maximal predictions from PLSR model occur at intermediate time (day 7) as there is a time lag for downstream effects of differentiation.